Comparison of isotropic, VTI and TTI reverse time migration: an experiment on BP anisotropic benchmark dataset

Shengwen Jin, Fan Jiang and Yiqing Ren, Halliburton Landmark, Houston, TX 77042, USA*
*(*Intern from Texas Tech University)*

Summary

Reverse time migration (RTM) propagates the source wavefield forward and receiver wavefield backward in time using the two-way wave equation. RTM has been extended from isotropic media to transversely isotropic (TI) media including vertical TI (VTI) and tilted TI (TTI) media. Explicit finite difference (FD) scheme and pseudo-acoustic wave approximation for TI media by simply setting shear wave velocity as zero caused some practical issues in stability, memory requirement, efficiency and artifacts, etc. These issues are discussed in this paper and comparison of isotropic, VTI and TTI RTM on BP anisotropic benchmark dataset is demonstrated.

Introduction

Reverse time migration (RTM) has been successfully applied to production imaging processing in recent years. It propagates source wavefield forward in time and the receiver wavefield backward in time to image the subsurface reflector (Baysal et al, 1983; McMechan, 1983; Whitmore, 1983). By using the two-way acoustic wave equation, RTM has no dip limitation. Also, it naturally takes into account both down-going and up-going waves and thus enables imaging of the turning waves and prism waves that are able to enhance the image of steep salt flank and other steeply dipping events with complex structures.

Seismic anisotropy, the variation of the propagation speed of seismic waves as a function of traveling direction, widely exists in sediments in many areas, such as Gulf of Mexico, western Africa and North Sea. Transverse isotropy (TI) is one of the most common anisotropy we are dealing with these days (Thomsen, 1986). Conventional isotropic RTM produces erroneous images and misposition of the dipping events in TI media. Rather than developing an accurate and very computationally expensive anisotropic elastic RTM, Alkhalifah (1998, 2000) started from dispersion relation and proposed a pseudo-acoustic approximation in TI media by setting shear wave velocity along the symmetry axis as zero. Based on Alkhalifah's pseudo-acoustic approximation, a number of variations of RTM have been developed to account for the vertical TI (VTI) media (Zhou et al., 2006a; Hestholm, 2007; Du et al., 2008). Assuming the symmetry axis is normal to the bedding and tilting the symmetry axis accordingly, extensions from VTI to RTM in tilted TI media (TTI) have been developed (Zhou et al., 2006b; Fletcher et al., 2009; Zhang and Zhang, 2008). Alternatively, Duveneck et al. (2008) derived a pseudo-acoustic VTI wave equation by setting vertical shear velocity as zero based on Hooke's law and the equation of motion. These formulations are related. They are equivalent if Thomsen's anisotropic δ is constant (Duveneck et al., 2008). Duveneck et al.'s approach is able to physically interpret the horizontal and vertical stress components. Besides the stability condition required by explicit finite-difference (FD) scheme, applying the pseudo-acoustic equation with simply setting shear wave velocity along the tilted symmetry axis as zero can cause numerical computation unstable in TTI media with strong lateral variations of tilted dip angle. Attempts have been made to stabilize the TTI equation and reduce the shear wave artifacts (Fletcher et al., 2009; Liu et al., 2009; Zhang and Zhang, 2009).

Computational cost and memory requirement somehow prevent the TTI RTM from imaging of a large size production data. In this paper, we will discuss several practical issues on stability, memory usage and artifacts behavior. Comparison of isotropic, VTI and TTI RTM on the BP 2007 TTI anisotropic benchmark dataset will be demonstrated.

Explicit finite-difference scheme

Explicit finite-difference scheme with 10[th] order in space and 2[nd] order in time is used to discrete the second derivatives of space and time, i.e.

$$
\begin{aligned}
&\frac{\partial^2 P}{\partial x^2} \cong \frac{1}{\Delta x^2} \\
&[c_1(P_{i-1}+P_{i+1}) + c_2(P_{i-2}+P_{i+2}) + c_3(P_{i-3}+P_{i+3}) \\
&+ c_4(P_{i-4}+P_{i+4}) + c_5(P_{i-5}+P_{i+5}) + c_6 P_i]; \\
&\frac{\partial^2 P}{\partial t^2} \cong \frac{P(t+\Delta t) - 2P(t) + P(t-\Delta t)}{\Delta t^2}
\end{aligned}
\qquad (1)
$$

where $P_{i-1,} P_i, P_{i+1}$ represent $P(x-\Delta x), P(x), P(x+\Delta x)$.

FD coefficients are

$c_1 = 1.66667, c_2 = -0.23809, c_3 = 0.03968, c_4 = -0.00496,$
$c_5 = 0.000317, c_6 = -2.92722.$

Stability condition

To make the numerical computation stable with explicit finite difference scheme, time interval has to be small enough to satisfy the stability condition. According to Lines et al. (1999), the stability condition for isotropic RTM is as follow:

$$\Delta t \le \frac{\Delta d_{\min}}{v_{\max}} \cdot \frac{2}{\sqrt{a}}; \qquad (2)$$
$$a = \sum_{m=-M}^{m=M} (|W_x| + |W_y| + |W_z|)$$

where $\Delta d_{\min} = \min(\Delta x, \Delta y, \Delta z)$ is the minimum grid spacing. The grid spacing is governed by maximum frequency, minimum velocity and the order of FD scheme (Dablain, 1986). $v_{\max}$ is the maximum migration velocity. *W* is the FD coefficient and *M* is the FD order in space. Using the 10^{th} order FD scheme of equation (1), a=20.48 for 3D case.

The stability condition for VTI RTM is similarly derived as follow:

$$a = \sum_{m=-M}^{m=M} \frac{1}{3}\left[(|W_x| + |W_y| + |W_z|)(2 + 4\varepsilon + \sqrt{1+2\delta})\right] \qquad (3)$$

where ε and δ are Thomsen's TI anisotropic parameters. For the FD scheme of 10^{th} order in space,

$$a = 6.826 * (2 + 4\varepsilon_{\max} + \sqrt{1+2\delta_{\max}}) \qquad (4)$$

Because the value of (4) is usually greater than 20.48, the time interval for VTI RTM is smaller than that of isotropic RTM with the same FD scheme.

In general with TTI media, we can derive the stability condition as follow:

$$\begin{aligned} &a = W(a_1 + a_2); \\ &a_1 = (1 + 2\varepsilon_{\max})(2 - b); \\ &a2 = \sqrt{1 + 2\delta_{\max}(1+b)}; \\ &b = \cos^2\theta \sin 2\phi + \sin 2\theta(\sin\phi + \cos\phi) \end{aligned} \qquad (5)$$

where *W* is the sum of absolute value of coefficients of the 10^{th} order FD scheme, i.e. *W*=6.826. θ and ϕ are tilted dip and azimuth in TTI media, respectively. When $\theta = 0$ and $\phi = 0$, it reduces to VTI media. When $\theta = 90^0$, it reduces to horizontal TI (HTI) media.

Memory requirement

Unlike the downward extrapolation based one-way wave equation migration (WEM), RTM propagates the wavefields in time. It requires huge memory to store full 3D wavefields and models of the media. Especially in VTI and TTI RTM, additional anisotropic model parameters (epsilon, delta, dip and azimuth) need to be taken into account. As compared with isotropic RTM, a pseudo-acoustic wave equation for VTI and TTI RTM requires an auxiliary wavefield during wave propagation. Table 1 lists the basic memory allocations for each approach.

Isotropic RTM	VTI RTM	TTI RTM
P(t-1)	*P(t-1)*	P(t-1)
P(t)	*P(t)*	P(t)
ΔP	ΔP	ΔP
Velocity	*Q(t-1)*	*Q(t-1)*
	Q(t)	*Q(t)*
	ΔQ	ΔQ
	Velocity	*Velocity*
	Epsilon	*Epsilon*
	Delta	*Delta*
		Dip
		Azimuth

Table 1: Memory allocations for isotropic, VTI and TTI RTM

In the above table, *P(t-1)* and *P(t)* represent the wavefield at the previous and current time, respectively. ΔP represents a summation of the spatial derivatives. *Q* is an auxiliary wavefield used in VTI and TTI RTM. Assuming the size of 3D volume is (nx, ny, nz) and a unit SIZE=nx*ny*nz, the memory usage is (4*SIZE)*4 bytes for isotropic RTM, (8*SIZE)*4 bytes for VTI RTM, and (9*SIZE)*4 bytes for TTI RTM. Epsilon, delta, dip and azimuth are treated as short integer. Apparently, VTI and TTI RTM require as twice of memory as isotropic RTM.

According to the above discussion, if we can increase the grid spacing and time interval, the number of grids and time steps will decrease resulting in faster computation and less memory usage. The following actions can be taken to improve the efficiency of RTM:

1) Higher-order FD scheme in both space and time to make the grid spacing and time step bigger.
2) Hybrid WEM and RTM solution to allow for large grid spacing and time step with the existing FD scheme (Luo and Jin, 2008).
3) Adaptive grid spacing according to the velocity distribution.

Noises and artifacts

Conventional RTM imaging condition produces strong low frequency background noises. Poynting vector (Yoon et al., 2004) and Laplacian filter (Yoon and Zhou, 2001) are two main solutions to effectively attenuate such kind of noise. In anelliptic media ($\varepsilon \ne \delta$), due to the pseudo-acoustic approximation on the elastic wavefield for VTI and TTI RTM, the diamond-shape artifacts of the SV wavefront is clearly present (see Fig. 1a). Such artifacts can be suppressed by placing the source in isotropic layers which is always the case for offshore data or adding a small isotropic box around the source (Duveneck et al., 2008) (see Fig. 1b). The strong variations of dip angle and azimuth in terms of the tilted axis of symmetry can cause TTI RTM to be unstable (Zhang and Zhang, 2009;

Flectcher et al., 2009). The SV wavefront triplications need to be removed to make the numerical computation stable (Tsvankin, 2001). By adding a shear wave velocity, it helps wave propagation not blow out, but the shear wave exists in forward propagation (see Fig. 1c). The imaging condition will take care of it to avoid the contamination of the image by shear wave. Figure 2 demonstrates that TTI RTM generates strong artifacts in the area with strong variation of tilted dip (see Fig. 2b) and produces stable and nice image after special handling of shear wave propagation (see Fig. 2c).

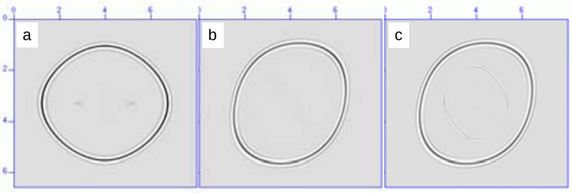

Figure 1: Snapshot of forward propagation. Background velocity is 3000 m/s, $\varepsilon = 0.25, \delta = 0.04, \theta = 40^0$. (a) Diamond shape on VTI RTM; (b) TTI RTM with isotropic box around source by setting SV velocity as zero; (c) TTI RTM by handling SV propagation.

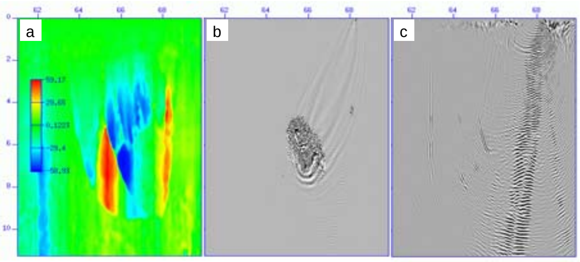

Figure 2: TTI RTM image of a single shot on BP TTI anisotropic model. (a) Tilted dip angle with strong lateral variation; (b) TTI RTM image with shear wave artifacts; (c) TTI RTM image after attenuating shear wave artifacts.

Experiment on BP anisotropic benchmark dataset

We performed the isotropic, VTI and TTI RTM on BP 2007 TTI anisotropic benchmark dataset created by an elastic finite difference modeling code. Although synthetic, the model is detailed so that with the noticeable exception of the surface multiples it looks very much like "real data" (Quotes from the release note of the dataset). Figure 3 shows the velocity in symmetry-axis direction, tilted dipping angle of anisotropy, and Thomsen's ε and δ models. Strong lateral variations of anisotropic properties exist on the models (see Fig. 3b and 3c). Rapid variation of tilted in three highlighted areas (see Fig. 3d) present challenges to TTI RTM. The images obtained from isotropic, VTI and TTI RTM are compared.

Figure 4 shows the comparison of images in area 1 of Fig. 3d with steep salt flank. As expected, the image of steep salt flank is mispositioned on isotropic RTM (see Fig. 4a) because the presence of anisotropy affects the positioning of dipping events. The VTI RTM produces a superior image of the steep salt flank, but some sediment events cross the salt boundary and penetrate into the salt body (see Fig. 4b). On TTI RTM image, the sediment events have nice terminations (see Fig. 4c). The missing salt boundary may be caused by the limited acquisition aperture. Figure 5 shows the comparison of images in area 2 with anticline structures. The amplitude varies on isotropic RTM image (see Fig. 5a). Discontinuities are clearly present and the deep anticline structures are distorted on the VTI RTM image (see Fig. 5b). The TTI RTM image perfectly matches the geological structure on the model. Figure 6 illustrates the comparison of images in area 3 with steeply dipping faults. On isotropic and VTI RTM images (see Fig. 6a and 6b), the faults are mispositioned and the image is poor between faults. In contrast, the faults on the TTI RTM image are very crispy and correctly positioned. Many detailed structures are well reconstructed (see Fig. 6c).

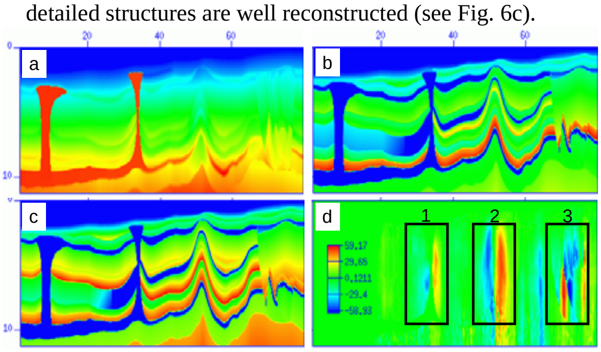

Figure 3: BP TTI anisotropic model. (a) Velocity model; (b) Thomsen's ε model; (c) Thomsen's δ model; (d) Tilted dip angle along the tilted symmetry-axis.

Conclusions

The TTI RTM produces superior image over isotropic and VTI RTM on the BP TTI anisotropic benchmark dataset, especially in those areas with strong variations of dip angle along the tilted symmetry-axis. Several issues such as stability condition, memory requirement as well as artifacts of shear wave triplications have been discussed for practical imaging application.

Acknowledgements

We acknowledge that the BP TTI Anisotropy Synthetic 2007 dataset was created by Hemang Shah and is provided courtesy of BP Exploration Operation Company Limited ("BP"). We also thank our colleagues Shiyong Xu, Steve Angelovich, Dan Grygier, Bob Basker, Margaret Dunckhorst and Craig Artley for their help.

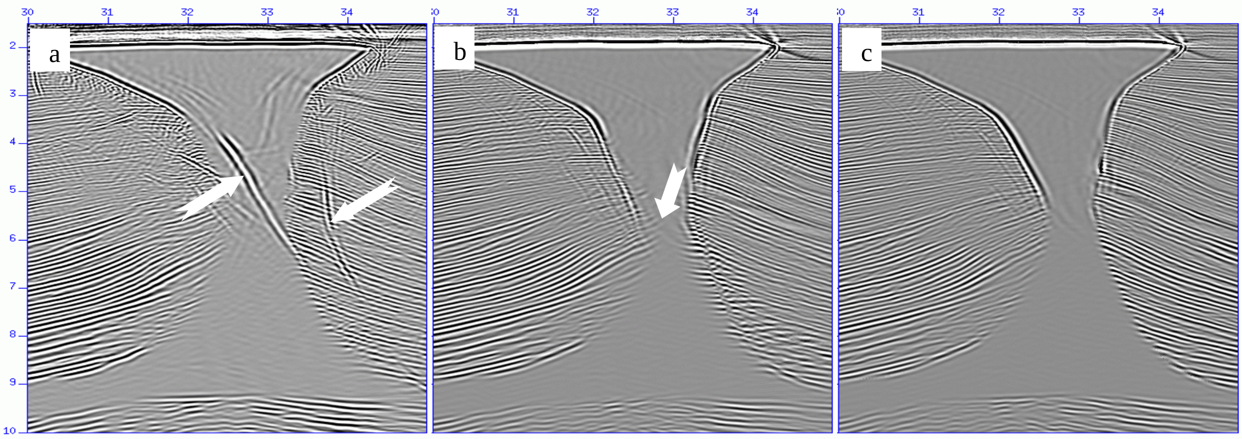

Figure 4: Comparison of isotropic RTM (a), VTI RTM (b) and TTI RTM (c) in area 1 of Fig. 3d.

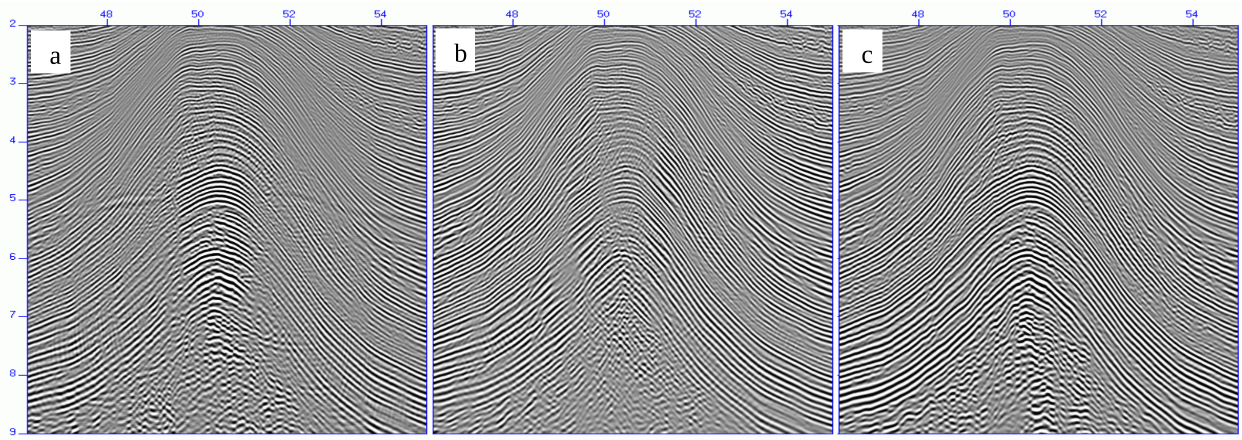

Figure 5: Comparison of isotropic RTM (a), VTI RTM (b) and TTI RTM (c) in area 2 of Fig. 3d.

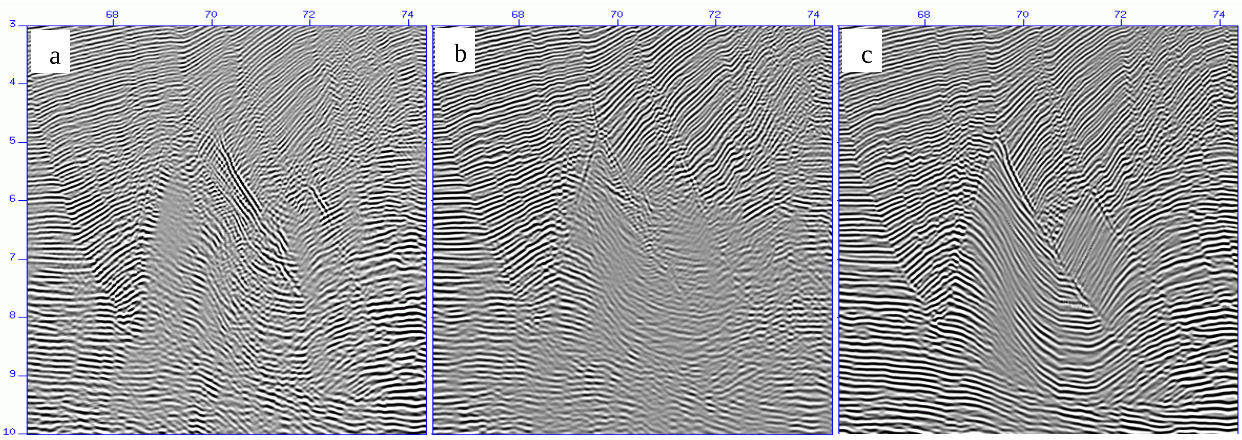

Figure 6: Comparison of isotropic RTM (a), VTI RTM (b) and TTI RTM (c) in area 3 of Fig. 3d.

EDITED REFERENCES

Note: This reference list is a copy-edited version of the reference list submitted by the author. Reference lists for the 2010 SEG Technical Program Expanded Abstracts have been copy edited so that references provided with the online metadata for each paper will achieve a high degree of linking to cited sources that appear on the Web.

REFERENCES

Alkhalifah, T., 1998, Acoustic approximations for processing in transversely isotropic media: Geophysics, **63**, 623–631, doi:10.1190/1.1444361.

Alkhalifah, T., 2000, An acoustic wave equation for anisotropic media: Geophysics, **65**, 1239–1250, doi:10.1190/1.1444815.

Baysal, E., D. D. Kosloff, and J. W. C. Sherwood, 1983, Reverse time migration: Geophysics, **48**, 1514–1524, doi:10.1190/1.1441434.

Dablain, M. A., 1986, The application of high-order differencing to the scalar wave equation: Geophysics, **51**, 54–66, doi:10.1190/1.1442040.

Du, X., R., Fletcher, and P. J., Fowler, 2008, A new pseudo-acoustic wave equation for VTI media: 70th Annual Conference and Exhibition, EAGE, Expanded Abstracts, H033.

Duveneck, E., and P. Milcik, P. M., Bakker, and C., Perkins, 2008, Acoustic VTI wave equations and their application for anisotropic reverse-time migration: 78th Annual International Meeting, SEG, Expanded Abstracts, 2186–2190.

Fletcher, R. P., X. Du, and P. J. Fowler, 2009, Reverse time migration in tilted transversely isotropic (TTI) media: Geophysics, **74**, no. 6, WCA179–WCA187, doi:10.1190/1.3269902.

Hestholm, S., 2007, Acoustic VTI modeling using high-order finite-differences: 77th Annual International Meeting, SEG, Expanded Abstracts, 139–143.

Lines, L. R., R. Slawinski, and R. P. Bording, 1999, A recipe for stability of finite-difference wave-equation computations: Geophysics, **64**, 967–969, doi:10.1190/1.1444605.

Liu, W., K. P., Bube, L. B., Zhang, and K., Nihei, 2009, Stable reverse-time migration in variable-tilt TI media: 71th Annual Conference and Exhibition, EAGE, Expanded Abstracts, P064.

Luo, M., and S. Jin, 2008, Hybrid one-way and full-way wave equation propagator and prestack migration: 78th Annual International Meeting, SEG, Expanded Abstracts, 2336-2340.

McMechan, G. A., 1983, Migration by extrapolation of time-dependent boundary values: Geophysical Prospecting, **31**, no. 3, 413–420, doi:10.1111/j.1365-2478.1983.tb01060.x.

Thomsen, L., 1986, Weak elastic anisotropy: Geophysics, **51**, 1954–1966, doi:10.1190/1.1442051.

Tsvankin, I., 2001, Seismic signatures and analysis of reflection data in anisotropic media: Elsevier Science Publ. Co., Inc.

Whitmore, N. D., 1983, Iterative depth migration by backward time propagation: 53rd Annual International Meeting, SEG, Expanded Abstracts, 827–830.

Yoon, K., K., Marfurt, and W., Starr, 2004, Challenges in reverse-time migration: 74th Annual International Meeting, SEG, Expanded Abstracts.

Youn, O. K., and H. Zhou, 2001, Depth imaging with multiples: Geophysics, **66**, 246–255, doi:10.1190/1.1444901.

Zhang, H., and Y. Zhang, 2008, Reverse time migration in 3D heterogeneous TTI media: 78thAnnual International Meeting, SEG, Expanded Abstracts, 2196–2200.

Zhang, Y., and H. Zhang, 2009, A stable TTI reverse time migration and its implementation: 79th Annual International Meeting, SEG, Expanded Abstracts, 2794-2798.

Zhou, H., G. Zhang, and R. Bloor, 2006a, An anisotropic acoustic wave equation for VTI media: 68th Annual Conference and Exhibition, EAGE, Expanded Abstracts, H033.

Zhou, H., G. Zhang, and R. Bloor, 2006b, An anisotropic acoustic wave equation for modeling and migration in 2D TTI media: 76th Annual International Meeting, SEG, Expanded Abstracts, 194–198.